ISSN 0036-0244, Russian Journal of Physical Chemistry A, 2024, Vol. 98, No. 9, pp. 1922–1926. © Pleiades Publishing, Ltd., 2024.

TO THE CENTENARY OF THE CHEMICAL THERMODYNAMICS LABORATORY OF MOSCOW STATE UNIVERSITY

Low-Temperature Heat Capacity of Zinc Tungstate Single Crystal

A. E. Musikhin[a],*, E. F. Miller[a], N. V. Gelfond[a], and V. N. Shlegel'[a]

[a] *Nikolaev Institute of Inorganic Chemistry, Siberian Branch, Russian Academy of Sciences, Novosibirsk, 630090 Russia*

**e-mail: musikhin@niic.nsc.ru*

Received November 3, 2023; revised November 7, 2023; accepted November 21, 2023

Abstract—The heat capacity of zinc tungstate was determined by relaxation calorimetry in the range of ~2.6–40 K. The heat capacity was extrapolated to zero temperature, and the characteristic Debye temperature at zero temperature was determined. The experimental heat capacities presented in the literature were estimated. The values of thermodynamic functions in the range 0–301 K were refined.

Keywords: relaxation calorimetry, heat capacity, thermodynamic functions, Debye temperature, cryogenic scintillators, zinc tungstate

DOI: 10.1134/S0036024424701024

INTRODUCTION

Molybdates and tungstates of divalent cations are promising materials for use in experiments on the recording of rare events, including the search for dark matter and detection of neutrinoless double beta decay, as well as for use as elements of lasers, various detectors, and sensors. For their use, especially as cryogenic scintillation bolometers, it is necessary to be able to obtain large single crystals with high chemical and optical quality, which should have a low intrinsic radio background and high energy resolution to ensure good selectivity in signal separation. This determines the wide interest of the scientific community in these objects. However, the heat capacity of these objects, especially in the range of low temperatures, is often not fully studied, and the values of thermodynamic functions at standard temperatures require refinement.

Zinc tungstate $ZnWO_4$ studied in this work meets the requirements described above and is both a laser and scintillation material and a promising cryogenic bolometer [1–5]. Its additional advantages are nonhygroscopicity and thermal and radiation stability. The structure of $ZnWO_4$ is known [6–8]; the crystal is monoclinic and belongs to the wolframite space group ($P2/c$). The melting point is 1474 K [9]. The literature presents the experimental heat capacities in the ranges 5–550 K [10, 11] and 81–301 K [12], as well as the enthalpy increment in the high-temperature range up to 1200 K [13]. The data presented in the literature have atypical behavior near zero and are not consistent with each other within the experimental uncertainty. This dictated the need to re-measure the data near zero to confirm the reliability of the literature data and refine the thermodynamic data at the standard temperature.

EXPERIMENTAL

Sample

High-quality zinc tungstate single crystals without optical defects were grown by the Czochralski method under conditions of low thermal gradients (LTG Cz). Within the framework of the method, the temperature gradients in the melt are limited to a level of no more than ~1 K cm^{-1}, the charge utilization factor reaches ~95%, and the grown crystals are of the highest quality.

Experimental Heat Capacity

The heat capacity of zinc tungstate was measured by the relaxation method using a PPMS-9+Evercool II complex for automated measurements of the physical properties of materials (Quantum Design, United States) at the "Center for Diagnostics of Functional Materials for Medicine, Pharmacology, and Nanoelectronics" of the St. Petersburg State University Science Park. A sample in the form of a rectangular parallelepiped with a base of 2.0 × 2.0 mm and a mass of 46.16 mg was prepared from the grown $ZnWO_4$ single crystal. The experimental heat capacity of the sample was measured both in the sample heating and cooling modes. Each series consisted of 27 points in the range ~2.6–40 K; partitioning along the temperature axis was performed on a logarithmic scale. The molar mass used was calculated from the formula $ZnWO_4$: 313.22 g mol^{-1}. The relative uncertainty of heat capacity measurements is ~2.0% or less, and its value

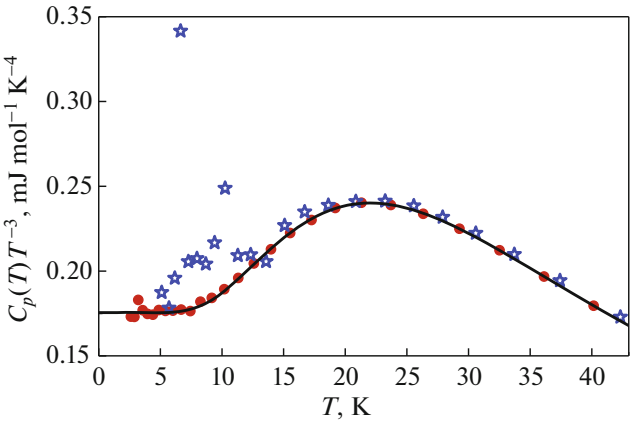

Fig. 1. Experimental data on the heat capacity of $ZnWO_4$: circles: data of this work; asterisks: data of [11]; solid curve: smoothed description of experimental data.

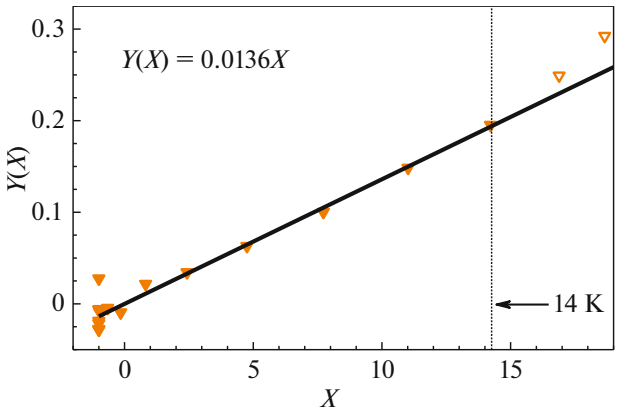

Fig. 2. Heat capacity of $ZnWO_4$ in the $Y(X)$ coordinates: triangles: experimental values; straight line: description of experimental points by the equation $Y(X) = 0.0136X$, whose validity region lies in the range 0–14 K.

depends on the temperature range in which the measurements are carried out [14]. The temperature uncertainty is 0.5%. The results of measurements are shown in Fig. 1 together with the data of [11].

RESULTS AND DISCUSSION

Extrapolation of Heat Capacity to Zero Temperatures

To calculate the integrated thermodynamic functions at the standard temperature, the obtained heat capacity data were extrapolated to zero, and the experimental $C_p(T)$ curve was smoothed. It was assumed that below 2.6 K the heat capacity of $ZnWO_4$ has no anomalous contributions.

According to Fig. 1, the heat capacity divided by the cube of temperature reaches a "shelf," which means that the experimental points of heat capacity near zero (below 8 K) belong to the region of validity of the Debye law. However, this region is characterized by increased experimental scatter, which makes the solution unstable when the starting and ending points are varied. To expand the experimental range from which the heat capacity will be extrapolated, a combination of the heat capacities of the Debye $C_D(T, \theta_D)$ and Einstein $C_E(T, \theta_E)$ models was used [15, 16]:

$$\frac{C_p(T)}{3Rn} = (1-\eta)C_D(T,\theta_D) + \eta C_E(T,\theta_E). \qquad (1)$$

Substituting the variables

$$Y(\theta_D) = \frac{C_p}{C_D} - 1 \quad \text{and} \quad X(\theta_D,\theta_E) = \frac{C_E}{C_D} - 1,$$

Eq. (1) can be transformed to a linear form:

$$Y(\theta_D) = \eta X(\theta_D,\theta_E). \qquad (2)$$

This procedure makes the solution more stable, thereby increasing the reliability of the search for parameters, and also gives an asymptotically correct description near zero.

The region of validity of (1) is defined as 0–14 K; the best description of the experimental data was achieved at parameter values $\theta_D = 403.1$ K, $\theta_E = 95.9$ K, and $\eta = 0.0136$. It was assumed that below 2.6 K the heat capacity of $ZnWO_4$ has no anomalous contributions. The result is shown in Fig. 2 in special coordinates $Y(X)$, the relative deviation of the experimental points is shown in Fig. 3 (triangles). The experimental point #3 at 3.21 K deviates statistically significantly (4.21%), so it was excluded from consideration in the calculation. The corresponding value of the characteristic Debye temperature at zero $\theta_D(0)$ for $ZnWO_4$ was 405 K.

Description of Heat Capacity in the Range 0–40 K

To describe the experimental heat capacity, we used an approach where the heat capacity is represented as the heat capacity of the Debye model and the sum of the heat capacities of the Einstein model. In this case, of $3n$ vibrational modes three acoustic modes are described by the Debye heat capacity $C_D(T, \theta_D)$ with a characteristic frequency θ_D, and the remaining modes are optical and described by the Einstein heat capacities $C_E(T, \theta_E)$ with the corresponding characteristic frequency θ_E. Here n reflects the number of atoms in the molecule and is equal to 6. Since the experimental heat capacity contains an anharmonic contribution, the sum of vibrational modes corresponding to the Einstein heat capacities will not

be limited by the condition $3(n-1)$. As a result, the equation for the heat capacity has the form:

$$\frac{C_p(T)}{3Rn} = \frac{1}{n}C_D(T,\theta_D) + \sum_{i=1}^{I} a_i C_{E,i}(T,\theta_{E,i}). \quad (3)$$

Here, the coefficient at the Debye heat capacity is 1/6, and the parameter $\theta_D = 222.9$ K corresponds to the previously found characteristic Debye temperature at zero $\Theta_D(0) = 405$ K. Then the contribution of the Debye heat capacity is subtracted from the total experimental heat capacity, and the result is described by a set of Einstein heat capacities $C_{E,i}(T)$. The parameters $\theta_{E,i}$ and a_i in Eq. (3) were found for $i = 1, 2, 3$ ($I = 3$) based on the minimum sum of squared deviations; the first characteristic Einstein frequency $\theta_{E,1} = 95.9$ K was determined earlier by extrapolating the heat capacity to zero and was not varied. The best result was achieved with the values of the parameters $\theta_{E,2} = 149$ K, $\theta_{E,3} = 314$ K; $a_1 = 0.01204$, $a_2 = 0.0356$, $a_3 = 0.2473$. The resulting heat capacity function is shown in Fig. 1 in the coordinates of C/T^3 vs. T (solid curve). The relative deviations of the obtained description from the experimental points are shown in Fig. 3 (circles), the relative standard deviation from the experimental data is 1.0% in the range of 2.6–11 K and 0.17% in the range of 11–40 K.

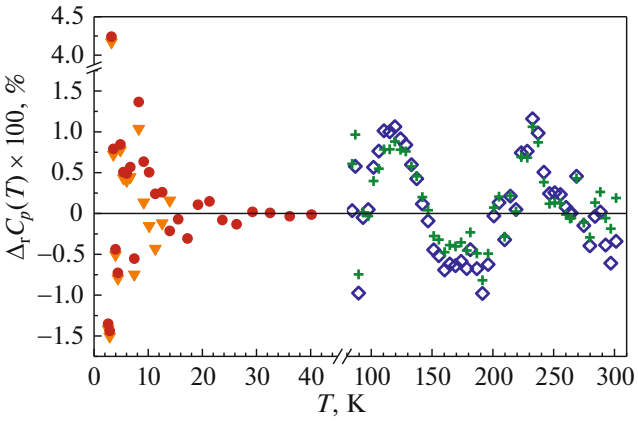

Fig. 3. Relative deviation of experimental values from the smoothed heat capacity (zero ordinate) for $ZnWO_4$: triangles: description by Eq. (1) in the range 2.6–14 K; circles and diamonds: description by Eq. (3) of the data of this work at 2.6–40 K and of the data of [12] at 81–301 K, respectively; pluses: smoothed description of the experimental heat capacity by a polynomial according to the data from [12]. The experimental point #3 at 3.21 K deviates statistically significantly (triangle and circle, 4.2%); it was excluded from consideration when finding the smoothed description.

Review of Literature Data on the Heat Capacity

We compared our results with those presented in the literature. The data of [11] systematically deviate from our data toward larger values, and these deviations range from 0.6 to 3.6% with anomalies of up to 94%. An analysis of the data of [11] showed that below 15 K there is an anomalous contribution; this is clearly visible, for example, in Fig. 1 (asterisks). Taking into account that the authors of [11] had problems with the zinc oxide impurity (in the earlier study [10], a $ZnWO_4$ sample contaminated with a ZnO impurity was used), it can be assumed that they did not achieve their goal in purifying the sample. It still contained some amount of impurities, including zinc oxide, which has an anomalous contribution to the Schottky-type heat capacity in the low-temperature region [17]. Thus, the heat capacity they obtained has an extraneous component and, as a consequence, is incorrectly normalized. The data of [12] were obtained by the adiabatic method in the range of 81–301 K. The high-quality pure sample studied in [12] was grown by the low-gradient Czochralski method. The data in [11] also systematically deviate from the data of [12] by 6–12%, which confirms that these data contain an extraneous heat capacity component associated with the possible presence of impurities in the sample. Since the enthalpy increment below 1200 K [13] was measured by the same team of authors as the heat capacity [10, 11], one can expect similar problems with the presented data. From the above it follows that the heat capacity and enthalpy increment data in the range of 300–1200 K require refinement.

Smoothed Description of Heat Capacity and Thermodynamic Functions in the Range of 0–301 K

When considering the data of this work along with the data of [12], another term with the parameters $\theta_{E,4} = 644$ K and $a_4 = 0.4357$ is added to Eq. (3). Thus, Eq. (3) with the found parameters is a function describing the smoothed heat capacity of $ZnWO_4$ in the range 0–301 K. The relative standard deviation of the experimental points from the obtained description in the range 81–301 K is 0.8%. The corresponding relative deviations are shown in Fig. 3 (diamonds); they repeat the deviations of the smoothed description of the heat capacity by the polynomial given in [12] (Fig. 3, pluses).

Based on the smoothed dependence $C_p(T)$ in the temperature range 0–301 K, the thermodynamic functions of zinc tungstate were calculated: entropy $S_p(T)$, enthalpy $\Delta H(T)$, and Gibbs free energy $\Delta G(T)$. The results are shown on Figs. 4 and 5.

The refined values of the thermodynamic functions of $ZnWO_4$ under standard conditions ($T = 298.15$ K, $p = 0.10$ MPa) were:

$$C_p^\circ(T) = 109.9 \pm 1.0 \text{ J mol}^{-1} \text{ K}^{-1},$$

$$S_p^\circ(T) = 116.9 \pm 1.3 \text{ J mol}^{-1} \text{ K}^{-1},$$

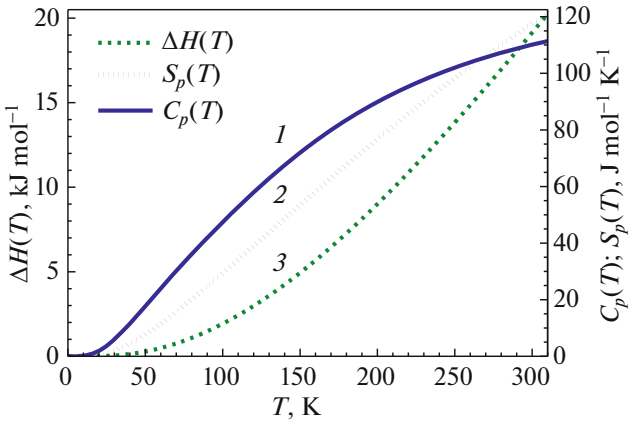

Fig. 4. Thermodynamic functions of $ZnWO_4$ in the range 0–301 K: (*1*) heat capacity $C_p(T)$, (*2*) entropy $S_p(T)$, and (*3*) enthalpy $\Delta H(T)$.

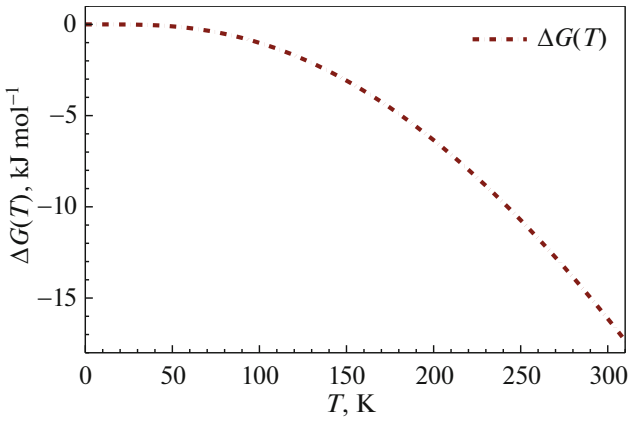

Fig. 5. Gibbs free energy $\Delta G(T)$ for $ZnWO_4$ in the range 0–301 K.

$$\Delta_0^{298.15}H(T) = 18.94 \pm 0.18 \text{ kJ mol}^{-1},$$

$$\Delta_0^{298.15}G(T) = -15.92 \pm 0.20 \text{ kJ mol}^{-1}.$$

CONCLUSIONS

An atypical behavior of the heat capacity below 15 K was discovered in the data of [11], which were obtained by measuring $ZnWO_4$ powder by the adiabatic method. To refine the values of the heat capacity near zero temperatures, an experimental study of the heat capacity of a zinc tungstate single crystal in the range of 2.6–40 K was carried out by the relaxation method, for the first time below 5 K. Using the experimental data, the heat capacity of $ZnWO_4$ was described in the region of low temperatures based on a physically substantiated equation and the Debye temperature at zero was calculated. No anomalous behavior of the heat capacity associated with the presence of any phase transitions was detected. A comparison with known data showed that the experimental heat capacity of [11] systematically deviates from both our heat capacity and that given in [12]. For example, the refined value of the heat capacity of $ZnWO_4$ at 298.15 K is 109.9 J mol^{-1} K^{-1}; it coincides with the value given in [12] within the experimental uncertainty and is 4.5% smaller than the value given in [11]. These facts allow us to conclude that the heat capacity of the sample of [11] has a contribution associated with the presence of impurity phases, possibly, zinc oxide, which, if present at a level of several percent, might not be detected on the analytical equipment of that time. The heat capacity of ZnO has an anomalous component associated with the Schottky effect in the low temperature region [16], whose contribution could give rise to the detected atypical behavior of heat capacity [11] near zero.

A smoothed description of the heat capacity in the range 0–301 K was obtained based on the joint consideration of data from this work and literature data [12]. The thermodynamic functions of zinc tungstate: entropy, enthalpy increment, and Gibbs free energy were calculated from these data.

FUNDING

This work was financially supported by the Russian Science Foundation, grant no. 23-79-00070.

CONFLICT OF INTEREST

The authors of this work declare that they have no conflicts of interest.

REFERENCES

1. Xin Wang, Ze Fan, Haohai Yu, et al., Opt. Mater. Express **7**, 1732 (2017). https://doi.org/10.1364/OME.7.001732
2. F. A. Danevich, V. V. Kobychev, S. S. Nagorny, et al., Nucl. Instrum. Methods Phys. Res., Sect. A **544**, 553 (2005). https://doi.org/10.1016/j.nima.2005.01.303
3. Z. Kowalski, S. M. Kaczmarek, M. Berkowski, et al., J. Cryst. Growth **457**, 117 (2016). https://doi.org/10.1016/j.jcrysgro.2016.06.043
4. P. Belli, R. Bernabei, Yu. A. Borovlev, et al., Nucl. Instrum. Methods Phys. Res., Sect. A **935**, 89 (2019). https://doi.org/10.1016/j.nima.2019.05.014
5. P. Belli, R. Bernabei, Yu. A. Borovlev, et al., Nucl. Instrum. Methods Phys. Res., Sect. A **1029**, 166400 (2022). https://doi.org/10.1016/j.nima.2022.166400
6. O. S. Filipenko, E. A. Pobedimskaya, N. V. Belov, et al., Sov. Phys. Crystallogr. **13**, 127 (1968).

7. P. F. Schofield, K. S. Knight, and G. Cressey, J. Mater. Sci. **31**, 2873 (1996). https://doi.org/10.1007/BF00355995
8. D. M. Trots, A. Senyshyn, L. Vasylechko, et al., J. Phys.: Condens. Matter **21**, 325402 (2009). https://doi.org/10.1088/0953-8984/21/32/325402
9. S. O'Hara and G. M. McManus, J. Appl. Phys. **36**, 1741 (1965). https://doi.org/10.1063/1.1703120
10. W. G. Lyon and E. F. Westrum, J. Chem. Thermodyn. **6**, 763 (1974). https://doi.org/10.1016/0021-9614(74)90141-4
11. C. P. Landee and E. F. Westrum, J. Chem. Thermodyn. **7**, 973 (1975). https://doi.org/10.1016/0021-9614(75)90161-5
12. P. A. Popov, S. A. Skrobov, A. V. Matovnikov, et al., Phys. Solid State **58**, 853 (2016). https://doi.org/10.1134/S1063783416040193
13. W. G. Lyon and E. F. Westrum, J. Chem. Thermodyn. **6**, 781 (1974). https://doi.org/10.1016/0021-9614(74)90142-6
14. J. C. Lashley, M. F. Hundley, A. Migliori, et al., Cryogenics **43**, 369 (2003). https://doi.org/10.1016/S0011-2275(03)00092-4
15. A. E. Musikhin, V. N. Naumov, M. A. Bespyatov, et al., J. Alloys Compd. **639**, 145 (2015). https://doi.org/10.1016/j.jallcom.2015.03.159
16. A. E. Musikhin, M. A. Bespyatov, V. N. Shlegel, et al., J. Alloys Compd. **802**, 235 (2019). https://doi.org/10.1016/j.jallcom.2019.06.197
17. W. N. Lawless and T. K. Gupta, J. Appl. Phys. **60**, 607 (1986). https://doi.org/10.1063/1.337455